

The Gastropod Fast Radiative Transfer Model for Advanced Infrared Sounders and Characterization of Its Errors for Radiance Assimilation

V. SHERLOCK

National Institute of Water and Atmospheric Research, Kilbirnie, Wellington, New Zealand

A. COLLARD

Met Office, Reading, United Kingdom

S. HANNON

University of Maryland, Baltimore County, Baltimore, Maryland

R. SAUNDERS

Met Office, Exeter, United Kingdom

(Manuscript received 16 October 2002, in final form 5 April 2003)

ABSTRACT

Principal aspects of the development of Gastropod, a fixed-pressure-grid fast radiative transfer model for the Atmospheric Infrared Sounder (AIRS), are described. Performance of the forward and gradient operators is characterized, and the impact of radiative transfer model errors on retrieval accuracy is quantified in a minimum-variance linear retrieval framework. The model error characteristics do not compromise the information content of channel subsets appropriate for use in operational data assimilation significantly, and retrieval accuracy is robust in realistic suboptimal retrieval scenarios. The fixed-pressure-grid regression model is, therefore, adequate for current data assimilation requirements. Errors in modeled water vapor line absorption do, however, limit the accuracy of retrievals using the full AIRS channel set, and accurate description of forward-model error correlations is essential for retrieval accuracy. Thus, despite recent advances, fixed-pressure-grid models have yet to demonstrate the required degree of accuracy in modeling water vapor line absorption. More accurate models will be required to exploit advanced sounder data to their full potential.

1. Introduction

Satelliteborne instruments form a major component of meteorological and climate observing systems. Requirements for improved weather prediction and improved understanding of natural and anthropogenic processes affecting climate have led to the development of advanced infrared spectrometers (Aumann and Pagano 1994) and interferometers (Chalon et al. 2001; Predina and Glumb 2000). These instruments have high spectral resolution, which will enable temperature and humidity profiles to be determined with higher accuracy and higher vertical resolution than is currently possible. The first of these advanced sounders, the Atmospheric Infrared Sounder (AIRS) was launched on *Aqua* in May of 2002.

The interpretation of the satellite measurements is not

trivial, however. Observed radiances are related to surface and atmospheric state variables (pressure, temperature, and absorbing gas abundances) indirectly, through the radiative transfer equation. In the case of absorption by a variable gas, this relationship may be highly nonlinear. Furthermore, the unconstrained inversion problem is ill conditioned or, in some cases, ill posed. Over the past decade, variational methods for data assimilation have been developed that address these problems specifically and allow radiances to be assimilated directly in weather forecast models (Eyre et al. 1993). Resulting improvements in the accuracy of analyzed and forecast fields testify to the major advances that have been made in the use of satellite data (Simmons and Hollingsworth 2002).

In direct radiance assimilation, a radiative transfer operator is used to predict observed radiances for a given a priori estimate of atmospheric state (i.e., forecast model fields). A statistically optimal estimate of the true atmospheric state is sought through minimization of dif-

Corresponding author address: V. Sherlock, National Institute of Water and Atmospheric Research, P. O. Box 14-901, Kilbirnie, Wellington, New Zealand.
E-mail: v.sherlock@niwa.cri.nz

ferences between observed and predicted radiances, subject to a constraint on departures from the a priori estimate of atmospheric state. The gradient of the radiative transfer operator with respect to elements of the atmospheric state vector (the adjoint or Jacobian) is required for this minimization procedure. The weights given to observations depend on the magnitude of observation errors, so error covariance matrices for instrumental noise (**E**), forward model error (**F**), and the a priori estimate of atmospheric state (**B**) must also be specified.

The radiative transfer model—comprising forward and gradient operators and an estimate of the error covariance matrix **F**—is, therefore, the key to extracting the information contained within the observed radiances. For this to be done in a timely fashion, allowing all relevant data to be included in a model forecast cycle, the forward and gradient radiative transfer calculations must be very fast (e.g., 0.01 seconds per field of view for radiance assimilation in the Met Office operational suite). Approximations must be made to achieve these processing times.

Fast radiative transfer models fall into two main categories—direct statistical models, which employ regression techniques (e.g., neural networks, empirical orthogonal function decomposition) to relate atmospheric state variables and radiances directly, and physically based models, which solve a polychromatic approximation of the radiative transfer equation (McMillin and Fleming 1976). The former class provides very rapid forward calculations, but an accurate analytic Jacobian capability has yet to be demonstrated (Saunders 2000).

Physically based models depend on rapid but accurate estimation of absorber optical depths. Regression-based prediction of optical depths on a fixed pressure grid (FPG) or fixed absorber overburden grid (FAO) are the most widely used approaches (McMillin et al. 1979, 1995). Garand et al. (1999) have applied a Goody band model to estimate effective monochromatic optical depths for filter radiometers.

Development of physically based regression models for the advanced satellite sounders dates from the work of Hannon et al. (1996), which gave rise to the Pressure-Layer Fast Algorithm for Atmospheric Transmittance (PFAAST) models for AIRS and the infrared atmospheric sounding interferometer (IASI). Matricardi and Saunders (1999) more recently developed the radiative transfer for IASI (RTIASI) model. Intercomparison of these first FPG fast models for IASI identified a number of shortcomings in the treatment of modeled water vapor absorption in the RTIASI model, and errors in modeled absorption in the water vapor (H_2O) ν_2 band were shown to compromise retrieval accuracy (Sherlock 2000a,b). Improved modeling of water vapor absorption was clearly required to reduce forward-model errors below instrumental noise levels—particularly the low AIRS instrumental noise levels in the the longwave window region and H_2O ν_2 band.

Model developments have continued in recent years. Matricardi et al. (2001) have developed a new set of predictors, giving marked improvements in model performance for AIRS, IASI, and current infrared filter radiometers. These developments are integrated in the FPG model known as Radiative Transfer for Television and Infrared Observation Satellite (TIROS) Operational Vertical Sounder (TOVS) (RTTOV-7; Saunders et al. 2002). Hannon and coworkers have pursued a hybrid FPG-FAO approach in the development of the AIRS radiative transfer algorithm (AIRS-RTA). Van Delst (2002) recently reported ongoing development of the FAO optical path transmittance (OPTRAN) model for AIRS.

The Gastropod development described here has sought to optimize FPG model formulation and predictors based on the results of the Sherlock (2000b) model intercomparison and subsequent predictor selection studies (Sherlock 2002). In the following sections, we describe the main choices made in the development of Gastropod. We characterize Gastropod forward-model and Jacobian errors and compare them with forward-model error characteristics published for the RTTOV-7 and AIRS-RTA models. We then examine the impact of forward-model errors on retrieval accuracy in the context of numerical weather prediction data assimilation. In doing so, we aim to provide a critical assessment of FPG fast-model performance that may serve as a reference for future fast-model developments.

2. Radiative transfer model development

a. Basic principles of the fast radiative transfer model

Given an estimate of atmospheric state (profiles of temperature and absorbing gas abundances) and surface properties (temperature and emissivity), the forward radiative transfer operator calculates the radiance spectrum that would be observed by a satelliteborne instrument. The radiances deduced from satellite observations are given by the convolution of the incident monochromatic radiation spectrum $R(\nu)$, at frequencies ν , with the instrument spectral response functions for the k instrument channels $I_k(\nu)$. However, full line-by-line radiative transfer and convolution calculations are too time consuming (10^2 – 10^3 seconds per field of view) for operational data processing and assimilation requirements, and most physically based fast radiative transfer algorithms—including Gastropod—use the polychromatic transmittance approximation and regression-based prediction of optical depths to achieve the computational speeds required (e.g., 10^{-4} seconds per channel per field of view for AIRS, assuming a subset of 100 channels is assimilated).

In this case, an approximate solution to the discretized radiative transfer equation (here, assuming a plane-parallel atmosphere of nonscattering gaseous absorbers in

local thermodynamic equilibrium, and specular reflection at the earth's surface) is sought in terms of convolved layer-to-space transmittances:

$$\begin{aligned} \tilde{R}_k &= \int R(\nu)I_k(\nu) d\nu \\ &\simeq \tilde{\epsilon}_k B_k^*(T_s)\tilde{\tau}_{N,k} + \sum_{i=1}^N B_k^*(\bar{T}_i)(\tilde{\tau}_{i-1,k} - \tilde{\tau}_{i,k}) \\ &\quad + (1 - \tilde{\epsilon}_k)\tilde{\tau}_{N,k}^2 \sum_{i=1}^N B_k^*(\bar{T}_i) \frac{\tilde{\tau}_{i-1,k} - \tilde{\tau}_{i,k}}{\tilde{\tau}_{i-1,k}\tilde{\tau}_{i,k}}. \end{aligned} \quad (1)$$

The three terms on the right-hand side of Eq. (1) describe the contributions to the upwelling radiance at the top of the atmosphere from surface and atmospheric thermal emission and surface reflection of downwelling atmospheric thermal emission, respectively; k is the instrument channel index; i is the layer index, running from 1 at the top of the atmosphere to N at the surface; $\tilde{\tau}_{i,k}$ is the convolved transmittance from the base of the layer i to space, with $\tilde{\tau}_{0,k} = 1.0$; \bar{T}_i is the mean temperature of the layer i ; T_s is the surface skin temperature; $B_k^*(\bar{T}_i)$ is an appropriate spectral mean of the Planck function for the channel k ; and $\tilde{\epsilon}_k$ is an appropriate spectral mean surface emissivity for the channel k . Advanced sounders' channel half-widths are on the order of 0.25 cm^{-1} , allowing these mean quantities to be approximated by the Planck function and the spectral emissivity at the channel central frequency, respectively. More complicated formulations are required for filter radiometers.

The effective layer-to-space transmittance of the absorber X_m , $\tau_{i,k}^{X_m}$, is defined in terms of the convolved total monochromatic transmittance for the set of absorbers $\{X_l\}$, $\tau_i(\nu; X_1, \dots, X_{l-1}, X_l)$,

$$\tau_{i,k}^{X_m} = \frac{\int \tau_i(\nu; X_1, \dots, X_{m-1}, X_m)I_k(\nu) d\nu}{\int \tau_i(\nu; X_1, \dots, X_{m-1})I_k(\nu) d\nu}, \quad (2)$$

ensuring effective optical depths are additive (convolved optical depths of individual gases are not additive), and thus giving

$$\tilde{\tau}_{i,k} = \prod_{m=1}^M \tau_{i,k}^{X_m} = \int \tau_i(\nu; X_1, \dots, X_M)I_k(\nu) d\nu. \quad (3)$$

To compute the effective transmittance for the gaseous absorber X , effective layer optical depths $d_{i,k}^X$ are predicted using regression relations:

$$d_{i,k}^X = -\ln\left(\frac{\tau_{i,k}^X}{\tau_{i-1,k}^X}\right) = \sum_j c_{i,k,j}^X Q_{i,k,j}^X, \quad (4)$$

where $c_{i,k,j}^X$ and $Q_{i,k,j}^X$ are the regression coefficients and predictands for the absorber X , the layer i , and the chan-

nel k . The effective layer-to-space transmittances and the convolved layer-to-space transmittance are then deduced recursively. Regression coefficients are derived from convolved transmittances calculated using a line-by-line radiative transfer model.

As described above, two vertical layering definitions are used for regression-based prediction of convolved layer-to-space transmittances: levels of fixed pressure or levels of fixed absorber overburden. The two methods were compared in a study by Hannon et al. (1996). Both methods were shown to give accurate predictions of atmospheric transmittances. The authors concluded that, although the FAO approach is probably ultimately capable of the greater degree of accuracy, layering requirements associated with the transformation to absorber overburden space complicate model implementation and contribute significantly (a factor of 2) to model run time. Based on these results, the Gastropod uses the simpler fixed pressure grid.

b. The regression scheme for the prediction of effective layer optical depths

The regression scheme adopted in Gastropod follows that of the PFAAST model (Hannon et al. 1996). This model was selected because of low forward-model errors in spectral intervals where water vapor absorption dominates (Sherlock 2000b). These error characteristics are attributed to two main features of the Hannon et al. (1996) methodology: the separate prediction of water vapor line and continuum absorption, and the use of weighted regression.

The separation of the water vapor line and continuum absorption gives several advantages: the different absorber abundance and temperature dependencies of the line and continuum absorption are modeled separately, allowing fewer predictors in both regressions, and the spectrally smooth nature of the continuum absorption on the scale of advanced-sounder spectral bandwidths allows the effective optical depth for the water vapor continuum (CTM) to be approximated by the monochromatic continuum optical depth at the channel central frequency and added to the gaseous line absorption contribution. The expression for the convolved layer-to-space transmittances becomes

$$\tilde{\tau}_{i,k} = \tau_{i,k}^{\text{CTM}} \prod_{m=1}^M \tau_{i,k}^{X_m}, \quad (5)$$

allowing corrections to the description of the water vapor continuum to be readily incorporated into fast models without the need for the computationally expensive recalculation of the line-by-line transmittances.

The climatic range of water vapor abundances can lead to marked departures from a linear variation of effective optical depth with layer water vapor content when the overhead column is optically thick (Hannon et al. 1996; Sherlock 2001a). However, regression co-

TABLE 1. Gastropod predictors for fixed gas, water vapor line, water vapor continuum, and ozone absorption, and associated basis functions. As defined in the text, i is the layer index and ref denotes the reference profile; X_i denotes layer mean temperature or layer mean mixing ratio, as appropriate. Thus T_r is the ratio of input and reference profile layer mean temperatures, W_r is the ratio of layer water vapor mixing ratios, and O_r is the ratio of layer mean ozone mixing ratios. The $Y_{z,i}$ basis functions are column overburden terms, defined by the ratio of pressure-weighted variables summed over the layers overlying the layer i . Weights dP_i and \bar{P}_i are given by the difference and the mean of the pressures at the upper and lower boundaries of the layer, respectively, and χ is the satellite zenith angle.

Gastropod predictors, release version 0.2.0				
Fixed	H ₂ O line	Ozone	H ₂ O continuum	Basis definitions
a	aW_r	aO_r	aW_r/T_r	$a = \sec(\chi)$
a^2	$(aW_r)^2$	$(aO_r)^2$	aW_r/T_r^2	$X_{r,i} = X_i/X_{\text{ref},i}$
T_r	$\sqrt{aW_r}$	$\sqrt{aO_r}$	aW_r^2/T_r^4	$dT_i = T_i - T_{\text{ref},i}$
T_r^2	$\sqrt[4]{aW_r}$	$aO_r dT$	aW_r^2/T_r	$X_{z,i} = \frac{\sum \bar{P}_k dP_k X_k}{\sum \bar{P}_k dP_k X_{\text{ref},k}}$
aT_r	$aW_r dT$	$\sqrt{aO_r dT}$	aW_r^2/T_r^2	$k = 1, i - 1$
aT_r^2	$\sqrt{aW_r dT}$	$a^2 O_r W_r$		
aT_z	$aW_r dT dT $	aO_z		$TZ_{z,i} = \frac{\sum \bar{P}_k dP_k T_k X_k}{\sum \bar{P}_k dP_k T_{\text{ref},k} X_{\text{ref},k}}$
aT_z/T_r	aW_z	$aO_r \sqrt{aO_z}$		$k = 1, i - 1$
	$(aW_z)^2$	$aO_r TO_z$		$dP_i = P_{i+1} - P_i$
	$\sqrt{aW_z}$			$\bar{P}_i = (P_{i+1} + P_i)/2$
	$\sqrt{aW_r W_r / W_z}$			

efficients should not be unduly influenced by data points corresponding to optically thick situations because they do not make significant contributions to simulated radiances. Weighting data accordingly, prior to regression, is key to achieving the required accuracy for the fast-model transmittance prediction scheme: in this study, the use of weighted regression for the prediction of water vapor line absorption gave twofold to tenfold reductions in forward-model errors, with maximum reduction in water vapor line centers. In converse, predictions in optically thick situations effectively constitute an extrapolation of the regression relations. In Gastropod radiative transfer calculations, the transmittance to space is set to zero if the effective layer-to-space optical depth for water vapor line absorption is greater than 5.2, to avoid gross errors in low-level Jacobians. A full discussion is given in Sherlock (2001a).

The regression model developed in this study makes further extensions to the model of Hannon et al. (1996). In an attempt to solve the difficulties in accurately modeling water vapor line absorption described above, early FPG fast models for the advanced sounders used different regression schemes for water vapor absorption, depending on the optical depth of the overhead column. However, this results in discontinuities in modeled Jacobians and is not to be recommended. Gastropod uses a single regression scheme for water vapor absorption. This scheme has required redefinition of the regression weighting function defined by Hannon et al. (1996) and is described in Sherlock (2001a).

Preliminary validation of Gastropod forward and Jacobian model predictions, using the water vapor line absorption predictors proposed by Hannon et al. (1996), highlighted errors in predicted water vapor line absorption for a class of atmospheres with structured (layered) humidity profiles in the upper troposphere (Sherlock et

al. 2002). A subsequent predictor selection study (Sherlock 2002) demonstrated that the $\sqrt{aW_r W_r / W_z}$ (see Table 1 for definitions) predictor proposed by Matricardi et al. (2001) is a lead predictor for water vapor line absorption in the 1400–1600 cm^{-1} range. The final set of water vapor line absorption predictors adopted for the version 0.2.0 release of the Gastropod model is defined and tabulated in Table 1. The predictor set proposed by Hannon et al. (1996) has been revised to include the $\sqrt{aW_r W_r / W_z}$ predictor. Redundant predictors have also been excluded, primarily to limit errors caused by predictor collinearity (Sherlock 2002).

Based on the results of a previous study of the vertical discretization required for FPG fast models for the advanced sounders (Sherlock 2001b), arithmetic means are used to estimate layer mean radiative properties; the vertical discretization of the fast model (AIRS 101 pressure levels) is sufficiently fine to ensure that no significant representativity errors are incurred (Sherlock 2000b, 2001b), and the use of an arithmetic mean gives a marked improvement in the speed of adjoint and Jacobian calculations over a weighted Curtis–Godson approximation.

Convolved transmittance data for the generation of the regression coefficients were calculated by author Hannon using the kcompressed atmospheric radiative transfer algorithm, (kCARTA), version 1.10 (Strow et al. 1998). The prelaunch AIRS spectral response function (which was available online at <http://asl.umbc.edu/pub/airs/srf/srftablesV10.hdf>) is assumed in convolutions. The transmittance database will be updated and regression coefficients will be regenerated once the true spectral response function is determined. Relevant characteristics of the transmittance database are summarized in Table 2.

TABLE 2. Principal characteristics of the UMBC convolved transmittance database.

Generating model		kCARTA (Strow et al. 1998)
Spectroscopy	Line parameters	High-Resolution Transmission Model (HITRAN) 98 (Toth H ₂ O lines)
	CO ₂ line mixing	Strow et al. (2003)
	H ₂ O continuum	Correlated <i>K</i> -distribution approximation (CKD) 2.4
Atmospheric absorbers	Fixed gases	All HITRAN gases except H ₂ O and ozone
	Fixed gas concentrations	<i>U.S. Standard Atmosphere, 1976</i> [CO ₂] × 370/330, [CH ₄] × 1.8/1.7
	Variable gases: H ₂ O, ozone	UMBC AIRS profile set (48)
Discretization	Vertical	101 AIRS pressure levels
	Spectral (kCARTA)	0.0025 cm ⁻¹
Convolution		Pure spectral response functions (no fringes), nominal 155-K frequencies

c. The Gastropod radiative transfer model

Over and above the modifications to the PFAAST regression scheme described above, the main reason for not adopting the PFAAST model as it stood was the fact that the corresponding adjoint and Jacobian code had not been developed, maintained, or distributed and there was no definite plan to do so.

Gastropod solves the clear-sky discrete radiative transfer equation, as formulated in Eq. (1). Standard adjoint techniques (Giering and Kaminski 1996) have been used to derive the tangent linear, adjoint, and *K* codes of the forward model. Specifically, the *K* code calculates the exact analytic Jacobians of the forward model by executing the sequence of adjoint code statements corresponding to each step of the forward algorithm. In addition, interface routines have been developed that allow profile input and Jacobian output on arbitrary (i.e., user defined) pressure levels.

The radiative transfer model does not currently include downwelling solar radiation or a prognostic infrared surface emissivity scheme (e.g., Sherlock and Saunders 2000) and does not allow for the treatment of cloud. These extensions are planned in upcoming work.

The input state vector currently comprises temperature, water vapor and ozone volume mixing ratios (with respect to the total number density of air molecules) as a function of pressure, surface pressure, surface skin temperature, and spectral emissivity for all channels. The mixing ratios of all other gaseous absorbers are assumed to be time invariant. The radiative effects of climatological variability of carbon dioxide, carbon monoxide, nitrous oxide, and methane (CO₂, CO, N₂O, and CH₄, respectively); errors in the specification of surface emissivity; unmodeled reflected downwelling solar radiation; and departure from local thermodynamic equilibrium must be included in estimates of the forward-model error covariance.

Gastropod is an open-source development. Software is distributed under the Gnu Lesser General Public License and at the time of writing could be downloaded from <http://gastro.sourceforge.net>. Regression coefficients for the AIRS instrument are also available from this site.

3. Characterization of forward-model and Jacobian errors

The accuracy of fast-model radiance simulations depends on the predictive accuracy and representativity of the underpinning regression model (referred to hereinafter as fast-model errors) and the accuracy of the line-by-line model transmittance calculations used to derive this model.

Fast-model errors are typically characterized by comparing predicted convolved transmittances, forward model radiances, and Jacobian calculations with reference line-by-line simulations. Forward-model and Jacobian error characterizations are presented here. They have the advantage of including errors from prediction of convolved transmittances, the polychromatic approximation, and representativity errors associated with the fast-model discretization of the radiative transfer equation (Sherlock 2000b). These characterizations are also directly related to the use of the model in data assimilation: fast-model errors should not make a significant contribution to the observation error covariance $\mathbf{R} = \mathbf{E} + \mathbf{F}$, and Jacobians must be modeled accurately if data are to be used optimally in assimilation (Watts and McNally 1988; Sherlock 2000a). Validation of convolved transmittances is described in Sherlock (2001a).

Although line-by-line calculations are based on the best physical description of atmospheric radiative transfer currently available, recent studies indicate that line-by-line modeling and representativity errors (formulation, spectroscopic parameter uncertainties, and—in the case of comparisons with observed spectra—nonlinearity of the radiative transfer problem) can be significant (Tjemkes et al. 2003). Corresponding contributions to the forward-model error covariance matrix are potentially much larger than the fast-model errors illustrated here.

a. Method

1) ESTIMATION OF THE FORWARD-MODEL ERROR COVARIANCE MATRIX

Convolved radiance spectra have been calculated (using Gastropod) at five zenith angles ($\chi = 0^\circ, 15^\circ, 30^\circ,$

45°, and 60°) for an independent set of 176 diverse atmospheric profiles from the European Centre for Medium-Range Weather Forecasts (ECMWF) 50-level numerical weather prediction model (Chevallier 1999) and were compared with convolved line-by-line radiances simulated using the kCARTA, version 1.10, model. Convolved radiances are converted to brightness temperatures (equivalent blackbody temperatures), and error statistics are estimated based on brightness temperature differences, because this has been shown to be the most appropriate noise metric for data assimilation (Sherlock 2000a, their appendix B). The error covariance estimate does not include errors associated with specification of surface emissivity; the specular reflection approximation or unmodeled surface reflection of downwelling solar radiation ($\bar{\epsilon} = 1$ is assumed in all radiative transfer calculations); variability of CO₂, CO, N₂O, or CH₄; line-by-line model; or nonlinearity errors.

The independent profile set is made up of 150 profiles randomly selected from a diverse set of representative atmospheric states and 26 profiles randomly selected from a set of extreme atmospheric states (Chevallier 1999). The sample set of atmospheres is, therefore, slightly biased toward extreme states but ensures that model performance is characterized in the widest possible range of situations. Statistical comparisons of the profile spaces spanned by the dependent and independent profile sets indicate that the dependent set generally spans the range of atmospheric states in the diverse profile set. However, profile extrema in temperature and humidity in the boundary layer and temperature extrema in the stratosphere in high-latitude profiles are underestimated in the dependent set.

Temperature and humidity profiles are dynamically and thermodynamically consistent in the independent profile set, but associated ozone profiles are drawn from climatological data. Physical correlations between temperature and ozone or humidity and ozone (and implicitly underpinning the fast-model regression) will not therefore be represented in the independent dataset, limiting its use for the validation of modeled ozone absorption; this validation is deferred to a later date.

2) ESTIMATION OF THE INSTRUMENTAL NOISE COVARIANCE MATRIX

The instrumental noise error covariance matrix \mathbf{E} assumed in the graphical comparisons illustrated below and in retrieval error characterization studies aims to provide a simple but realistic lower bound for advanced infrared sounder instrumental noise levels, and, hence, to provide the most demanding test of fast-model performance. The instrumental noise per channel at a 250-K scene temperature, $\text{NE}\Delta T(\nu, T_B = 250)$, is defined as

$$\text{NE}\Delta T(\nu, 250) = \begin{cases} 0.2 \text{ K} & \nu < 800 \text{ cm}^{-1} \\ 0.1 \text{ K} & \nu \in [800:2400] \text{ cm}^{-1} \\ 0.2 \text{ K} & \nu > 2400 \text{ cm}^{-1}, \end{cases}$$

based on AIRS laboratory performance tests (Morse et al. 1999) and in-orbit noise values presented by T. Pagano at the July 2002 AIRS Science Team meeting.

For any given radiance simulation, the instrumental noise is scaled to the channel scene temperature T_B :

$$\text{NE}\Delta T(\nu, T_B) = \frac{\left. \frac{\partial B(\nu, T)}{\partial T} \right|_{T=250\text{K}}}{\left. \frac{\partial B(\nu, T)}{\partial T} \right|_{T=T_B}}, \quad (6)$$

where ν is the channel central wavenumber and $B(\nu, T)$ is the Planck function as defined previously. Because no significant interchannel instrumental noise correlations were to be expected (Barnet and Susskind 1999), a diagonal instrumental error covariance matrix is assumed.

3) CHARACTERIZATION OF JACOBIAN ERRORS

It is difficult to define any single scalar figure of merit that completely characterizes the accuracy of modeled Jacobians (channel by channel) in a manner relevant to the retrieval problem. In this study, Jacobian errors are characterized by the Garand measure of fit (Garand et al. 2001):

$$\begin{aligned} & \text{(Garand measure of fit)}_k \\ & = 100 \times \sqrt{\frac{\sum_l (H'_{k,l} - H'_{k,l,\text{ref}})^2}{\sum_l H_{k,l,\text{ref}}^2}}, \quad (7) \end{aligned}$$

where k is the channel (wavenumber) index, l is the profile element (atmospheric state vector) index, $H(\mathbf{x})$ denotes the forward model; a prime denotes the derivative with respect to the state vector \mathbf{x} , and ref denotes reference Jacobians calculated from line-by-line radiance simulations. A Garand measure of fit of ≤ 10 is generally accepted as being indicative of well-modeled Jacobians, and a measure of fit of ≥ 25 is considered to be indicative of serious errors in modeled Jacobians. The measure of fit can generally be thought of as the percent error in modeled Jacobians in the region where $|H'|$ is maximum; clearly these Jacobian elements must be modeled accurately if any reliable assimilation or retrieval is to be performed.

The generation of line-by-line Jacobians is a very computationally intensive procedure. The results presented here are based on a reference set of finite-difference Jacobians (temperature ± 0.05 K, water vapor mixing ratio $\pm 1\%$) generated for the dependent profile set using the kCARTA model (Sherlock 2002). These Jacobian measures of fit should characterize Gastropod model performance generally because only modest forward-model error inflation occurs on passing from the dependent to independent profile sets (see below). As an alternative, results can be interpreted in terms of a

lower bound for Jacobian measures of fit for an independent profile set.

Jacobian fitting characteristics are summarized by the minimum, maximum, and upper quartile of the Garand measure of fit for each channel. Separate summations over the temperature and humidity components of the state vector are used to characterize errors in modeled temperature and humidity Jacobians independently. A threshold is applied, and only Jacobians for which $\max |H'| > 0.05$ are included in statistics.

4) INFORMATION CONTENT AND CHANNEL SELECTION

Assimilation of all advanced infrared radiance data (i.e., thousands of channels) is computationally intensive and inefficient, because the number of independent pieces of information contained in the data is much fewer than the number of channels. Thus, in practice, data from a reduced subset of channels (typically on the order of 100 channels) will be assimilated. These channel subsets will usually be determined from an analysis of measurement information content for a range of atmospheric states and representative a priori error covariances, following the method proposed by Rodgers (1996).

The impact of forward-model error on channel selection and measurement information content is, therefore, examined through comparison of an “ideal” channel subset—a set of 130 channels selected using the method of Rodgers (1996) and assuming a diagonal observation error covariance with standard deviations σ of 0.1 K for all channels—and an “actual” channel subset—a set of 130 channels selected based on actual estimates of observation error covariance matrix. The first of the two channel subsets is ideal in two senses: all absorption regimes and absorbing species would be equally well modeled and forward-model errors would not have a marked spectral dependence; a spectrally invariant observation error covariance matrix is often assumed in channel selection studies, and it is of interest to know whether this assumption is adequate or whether one needs to specify forward-model errors more accurately.

The sampling characteristics of the two channel subsets are described here. The impact on retrieval accuracy is quantified in section 4.

b. Radiative transfer model error characteristics for the CO₂ ν_2 and ν_3 bands and the atmospheric window regions

Forward-model errors for the 650–975 cm^{-1} interval are traced as a function of channel central wavenumber in Fig. 1. Instrumental noise levels are indicated for a representative range of scene temperatures by the shaded gray zone for comparison, although it should be recalled that the diagonal elements of the observation error

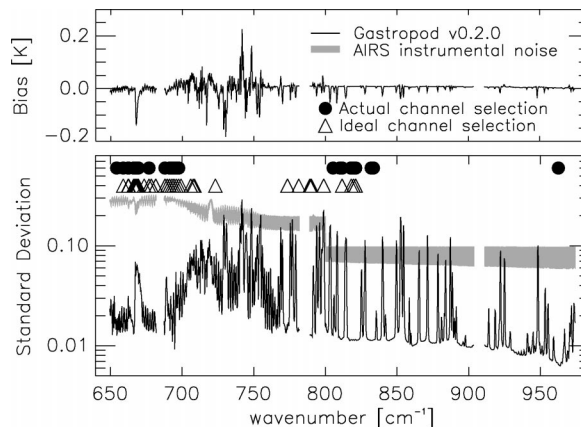


FIG. 1. Gastropod forward-model-error characteristics, channel subset sampling characteristics, and lower-bound estimates of AIRS instrumental noise levels for a representative range of scene temperatures for the 650–975 cm^{-1} wavenumber interval (AIRS bands 7–12).

covariance matrix are given by the sum of the squares of the standard deviations $\mathbf{R}_{k,k} = \sigma_{\mathbf{E},k}^2 + \sigma_{\mathbf{F},k}^2$. Ideal and actual channels subsets are indicated with open triangles and filled circles, respectively.

Overall model performance is good. With the exception of some channels in the 700–760 cm^{-1} interval, the 667 cm^{-1} CO₂ Q branch, and isolated water vapor lines in the window region, biases are less than 0.02 K. In a similar way, standard deviations are significantly lower than instrumental noise levels across the entire spectral interval, except in the 730–760 cm^{-1} interval and in water vapor line centers in the window region ($\nu > 780 \text{ cm}^{-1}$).

Forward-model errors for the independent set are generally robust. Error increases associated with the passage from the dependent to the independent profile set are modest ($\leq 30\%$, not shown). There is no substantial change in error statistics on exclusion of profiles that constitute an extrapolation of the regression relations or on exclusion of the set of 26 extreme profiles in the 176 profile set. Nor is there any marked dependence on satellite zenith angle or atmospheric state, with three exceptions: the largest biases and standard deviations in the 730–760 cm^{-1} interval are associated with errors in modeled water vapor line absorption (in the presence of interfering absorbing species, CO₂ and ozone) that depend on satellite zenith angle, maximum errors in the window region occur in water vapor line centers in humid atmospheres, and standard deviations in the high peaking CO₂ absorption bands—the 667 cm^{-1} and 720 cm^{-1} CO₂ Q branches—are reduced to less than 0.05 K on exclusion of high-latitude profiles for which stratospheric temperatures constitute an extrapolation of the regression relations (bias is attributed to differences in profile extrapolation above 0.1 hPa).

Jacobian error characteristics for the 650–975 cm^{-1} interval are illustrated in Fig. 2. Temperature Jacobians

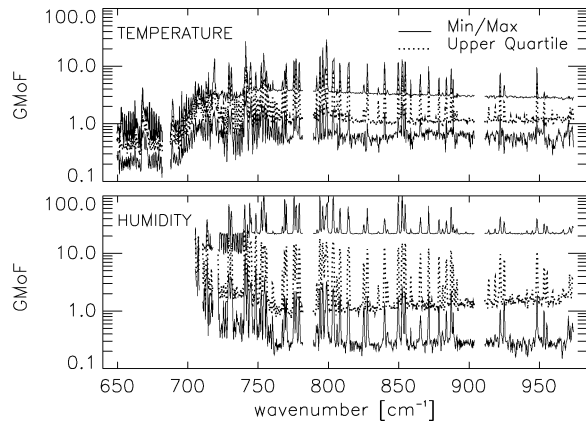


FIG. 2. Characterization of the accuracy of Gastropod temperature and humidity Jacobians on the 650–975 cm^{-1} interval, using the Garand measure of fit (GMoF).

are modeled well across the entire interval for all profiles. The largest errors occur in water vapor line centers but do not generally exceed a Garand measure of fit of 10. Elsewhere, Jacobians are considerably better modeled, with Garand measures of fit of 3 or less. Humidity Jacobians are also modeled well in most cases. Garand measures of fit are 10 or less for all channels for 75% of profiles. Again, the largest errors occur in line centers—elsewhere Garand measures of fit are on the order of 2 or less. Maximum Garand measures of fit are generally on the order of 20 and occur in dry atmospheres (where a small absolute error in modeled Jacobians gives a large relative error). However, maximum measures of fit in line centers exceed 40.

Similar model performance is obtained in the CO_2 ν_3 band (2220–2390 cm^{-1}). Forward-model standard deviation and temperature Jacobian results are reproduced in Fig. 3 for reference. Slightly higher standard deviation and Jacobian errors are apparent at the band head (~ 2380 cm^{-1}) and are associated with modeled absorption in the vicinity of the tropopause.

Forward-model errors do not significantly affect channel selection and measurement information content. The most significant modifications to channel selection, which occur when the true observation error covariance is taken into account (the modification to sampling in the CO_2 ν_2 and ν_3 bands and the shift in sampling to higher wavenumbers in the window region), are principally due to assumed instrumental noise levels rather than to forward-model errors. In the two instances in which forward-model errors are comparable to or greater than instrumental noise levels and could potentially affect information content (i.e., the 730–760 cm^{-1} interval and water vapor line centers in the window region), no channels are selected in either set. Thus, providing absorption in selected channels is adequately modeled, the penalty for excluding these poorly modeled channels from an assimilation set is negligible be-

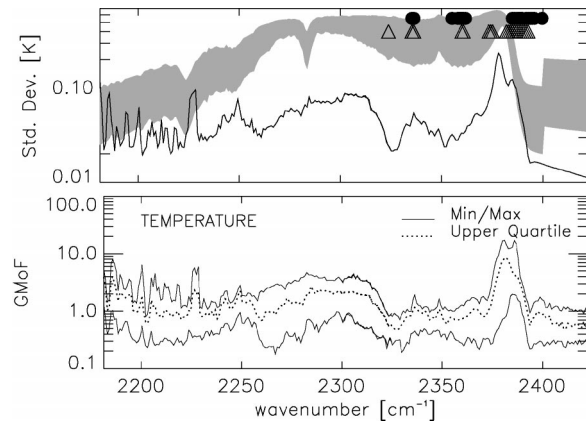


FIG. 3. Characterization of Gastropod forward-model and Jacobian estimates for the 2200–2400 cm^{-1} interval (AIRS bands 2B and 1B). Symbols and lines in the standard deviation plot are as defined in Fig. 1.

cause the additional information they would provide is small.

c. Radiative transfer model error characteristics for the H_2O ν_2 bands

Forward-model errors for a representative subinterval of the H_2O ν_2 band (1330–1630 cm^{-1}) are illustrated in Fig. 4. Beyond 1380 cm^{-1} , biases are generally low—on the order of 0.05 K in some line centers and considerably less elsewhere. However, significantly higher biases (and high standard deviations) are observed in some channels at wavenumbers less than 1380 cm^{-1} . These errors are associated with modeled water vapor line absorption in the presence of interfering methane absorption and exhibit a satellite zenith angle dependence.

Forward-model-error standard deviations range between 0.02 and 0.2 K. Minimum errors are associated with channels in the wings of water vapor lines. Max-

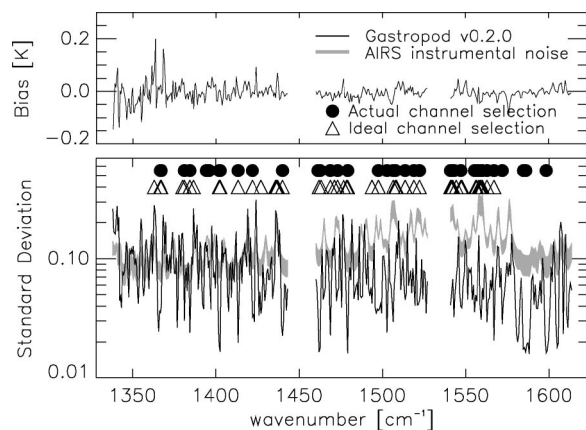


FIG. 4. Same as Fig. 1, but for the 1330–1630 cm^{-1} wavenumber interval (AIRS bands 03, 4B, and 4A).

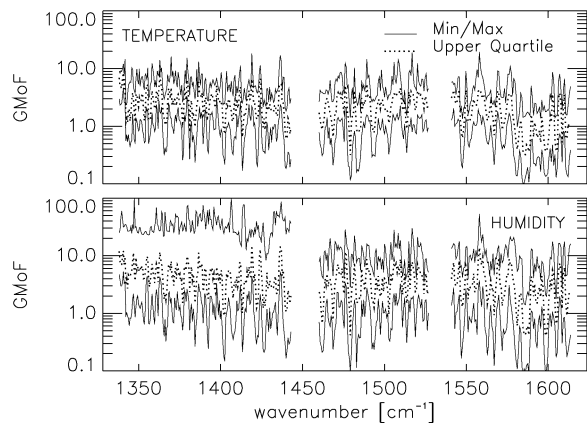


FIG. 5. Same as Fig. 2, but on the 1330–1630 cm^{-1} interval.

imum errors occur in water vapor line centers, and their magnitude tends to decrease across the spectral interval. As before, error increases associated with the passage from the dependent to the independent profile set are modest ($\leq 30\%$), there are no significant changes in error statistics on exclusion of extreme profiles, and forward-model errors do not show any marked dependence on atmospheric state or satellite zenith angle, other than the case noted above.

The low AIRS instrumental noise levels across the spectral interval pose challenging requirements for fast-model accuracy. In the 1330–1450 cm^{-1} interval, fast-model errors are only less than assumed instrumental noise levels in the wings of lines. In the 1450–1630 cm^{-1} interval, fast-model errors are less than or comparable to assumed instrumental noise levels for a wider range of absorption regimes, because of improved modeling of absorption in line centers and higher instrumental noise levels at lower scene temperatures.

Corresponding Jacobian errors for the 1330–1630 cm^{-1} subinterval are illustrated in Fig. 5. Temperature Jacobians are modeled well, with Garand measures of fit of 10 or less for all profiles and all wavenumbers in the interval. As before, the largest errors occur in water vapor line centers. Between lines, fits are considerably better, with measures of fit of 3 or less. A similar spectral structure is evident in the fitting errors for humidity Jacobians. Here, Garand measures of fit are less than 10 for 75% of profiles at all wavenumbers across the spectral interval. For wavenumbers greater than 1450 cm^{-1} , maximum Garand measures of fit rarely exceed 15, and fits in line wings are generally significantly better, with measures of fit of 5 or less. Maximum errors at wavenumbers less than 1380 cm^{-1} are generally on the order of 20–40 and are associated with dry atmospheres. Gross errors are observed in some line centers.

Because forward-model errors and instrumental noise levels are comparable in magnitude there are significant modifications to channel selections when the true observation error covariance is taken into account. In the 1350–1480 cm^{-1} interval, the ideal channel selection

spans several absorption lines while the actual channel selection remains constrained to the wings of lines. There is also a shift in sampling in the actual channel set to higher wavenumbers, exploiting improved modeling of tropospheric water vapor absorption in the H_2O ν_2 band center.

Poor forward-model-error characteristics in channels associated with interfering methane absorption ($\nu < 1380 \text{ cm}^{-1}$) preclude their use for data assimilation. This fact is not restrictive in the current development, because errors associated with the fixed-gas assumption necessitate their exclusion, irrespective of the accuracy of modeled water vapor absorption.

d. Error correlation

The discussion above has focused on forward-model-error standard deviations. Forward-model-error correlation structures are important and may need to be taken into account, particularly in spectral intervals in which forward-model error makes the dominant contribution to the observation error covariance matrix.

There is a high degree of forward-model-error correlation between channels within the CO_2 ν_2 and ν_3 absorption bands, and there are high correlations between the two bands. However, corresponding contributions to the off-diagonal elements of the full observation error covariance matrix are small, because instrumental noise levels are significantly higher than forward-model errors in these spectral intervals.

In a similar way there is a high degree of forward-model-error correlation between channels within the window regions and within the H_2O ν_2 band. The only significant, corresponding contributions to the off-diagonal elements of the full observation covariance matrix are due to correlations between channels located in water vapor line centers. A high degree of correlation is found between such channels within the window regions and within the H_2O ν_2 band, and between such channels in the window regions and the 1200–1400 cm^{-1} interval of the H_2O ν_2 band.

It was noted above that Jacobian errors and forward-model errors are correlated—large Jacobian errors occur in channels for which forward-model errors are largest—as is to be expected. Further, because regression-model errors depend on the absorption regime and there are only a limited number of predictors in the regression, Jacobian error structures are expected to be correlated between channels with similar absorption characteristics. Examination of Jacobian errors for selected profiles shows this to be borne out in practice.

e. Comparison with current fast-model-error characterizations

An equivalent forward-model-error characterization has been performed for the FPG RTTOV-7 AIRS fast model using a 117-profile subset of the 176 diverse-

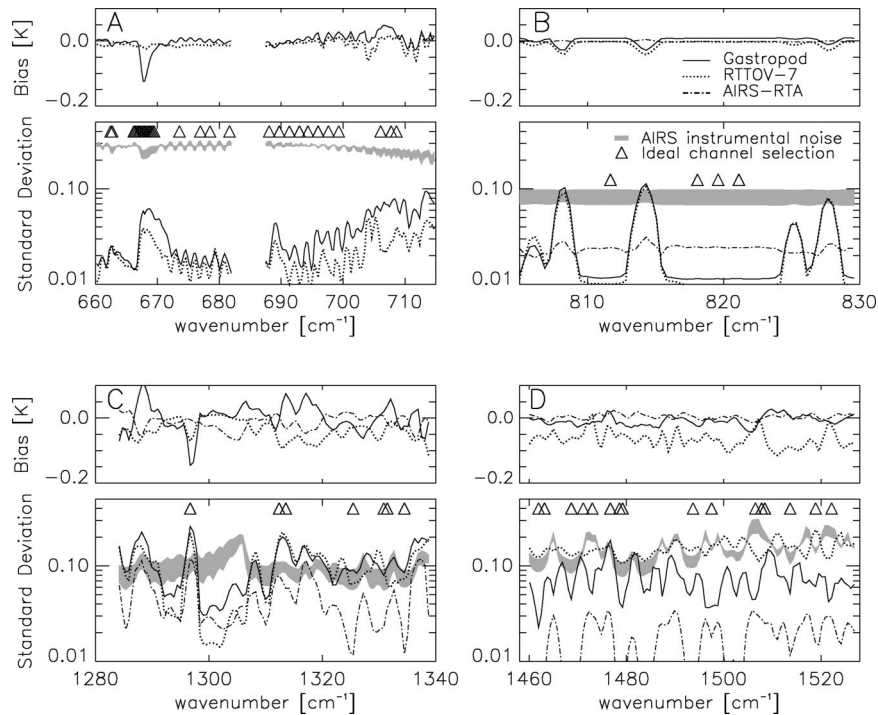


FIG. 6. Comparison of forward-model errors for the RTTOV-7 and Gastropod fixed-pressure-grid models on representative spectral subintervals of (a) the CO_2 ν_2 band, (b) the longwave atmospheric window region, and (c), (d) the H_2O ν_2 band (AIRS bands 4C and 4B, respectively). Forward-model-error characteristics of the AIRS-RTA FPG-FAO hybrid model are illustrated for reference on subintervals where water vapor is the principal absorber. All data have been smoothed with a three-point filter for visual clarity.

profile set (Matricardi et al. 2001; Saunders et al. 2002). These results are reproduced and compared with Gastropod forward-model errors for four representative spectral intervals in Fig. 6.

The RTTOV-7 regression scheme gives more accurate simulations—lower standard deviations¹ in the CO_2 absorption bands (Fig. 6a), but this result is not of major practical significance for data assimilation applications because other sources of error (principally instrumental noise) are predominant in these spectral intervals.

The error characteristics of the two models are very similar in the atmospheric window regions (Fig. 6b)—notably neither one models water vapor line absorption adequately—however, significant differences in model performance are found in the H_2O ν_2 band. At wavenumbers less than 1400 cm^{-1} (Fig. 6c) the forward-model standard deviations are comparable but Gastropod maximum biases are greater than RTTOV-7 maximum biases. At wavenumbers greater than 1400 cm^{-1} (Fig. 6d), RTTOV-7 model performance is poorest—standard deviations are comparable with instrumental

noise at all wavenumbers (i.e., even between absorption lines) and biases range from -0.05 to -0.1 K .

We have performed a range of tests described in detail in Sherlock (2002) using the Matricardi et al. (2001) water vapor line absorption predictors in regressions with the University of Maryland, Baltimore County (UMBC) dependent profile set. However, we do not reproduce the RTTOV-7 error characteristics (bias, standard deviation) in the $1400\text{--}1600\text{ cm}^{-1}$ interval, and, in fact, errors do not differ significantly from those described here for the Gastropod model. This, combined with the substantial increase in error reported by Matricardi et al. (2001) on passing from the dependent to the independent profile set, tends to call the representativity of the RTTOV-7 dependent profile set and/or model formulation [prediction of combined water vapor line and continuum absorption and absence of dedicated predictors for foreign continuum absorption (M. Matricardi 2003, personal communication)] into question. A single predictor, aW_r^2/W_z , in the Matricardi et al. (2001) set gives marked reductions in Gastropod maximum biases in the $1200\text{--}1400\text{ cm}^{-1}$ interval. However, because these maxima are generally associated with interfering methane absorption and because this predictor was not a significant predictor in regressions in other channels or spectral intervals, it was not included in the Gastropod predictor set.

¹ Note that the RTTOV-7 error characterization does not include vertical discretization (quadrature) errors, which are significant in subintervals A and D for the RTTOV-7 43-level pressure grid (Sherlock 2001b).

Independent validation results for the AIRS radiative transfer algorithm (Strow et al. 2003), based on a set of 212 TOVS Initial Guess Retrieval (TIGR) profiles, indicate considerably better model performance than either Gastropod or RTTOV-7 in water vapor line centers in the longwave window region and the $\text{H}_2\text{O } \nu_2$ band. With the exception of some channels in the 1250–1380 cm^{-1} and 1575–1625 cm^{-1} intervals, the AIRS-RTA model errors reported are of less than or on the order of 0.05 K throughout these spectral intervals. Although the error characterizations cannot be rigorously compared because of the different profile sets used in model-error characterization, AIRS-RTA error characterizations are traced for reference for subintervals B, C, and D, where water vapor is the principal absorber.

The AIRS-RTA model performance is achieved principally through the use of the FAO method for water vapor absorption and channel-specific sets of water vapor line absorption predictors. Thus, the results of Strow et al. (2003) indicate that water vapor absorption can be modeled to a high degree of accuracy, albeit with a notable increase in model complexity.

Full quantitative Jacobian error characterizations have not been performed for either model to date.

4. Impact of radiative transfer model errors on retrieval accuracy

In operational data assimilation, both accuracy and computational efficiency are crucial. The latter is a particular issue for the advanced infrared sounders, with their many thousands of channels. Redundancy will typically be minimized through assimilation of a much reduced subset of channels with maximum information content, as discussed in section 3. Further gains in computational efficiency will generally be sought through a diagonal approximation to the observation error covariance matrix, enabling rapid calculation of the associated matrix inverse [a full matrix inverse requires $O(N^3)$ floating point operations (flops) for N channels, as compared with $O(N)$ flops in the diagonal case].

Radiative transfer errors have been characterized in detail for the Gastropod model in the preceding section. Although performance is generally acceptable, modeled absorption in water vapor line centers does not meet the usual criteria for model accuracy, that is, forward-model standard deviations significantly lower than instrumental noise levels and Jacobian measures of fit of 15 or less for all profiles. Furthermore, corresponding error correlations make a significant contribution to the off-diagonal elements of the observation error covariance matrix. However, examination of the spectral sampling characteristics of the ideal channel subset shows many selected channels lie in the wings of absorption lines, where model performance is adequate.

In this section we quantify the impact of these radiative transfer model errors on retrieval accuracy in an operational data assimilation context, using a linear min-

imum variance analysis. Information loss caused by forward-model error is quantified for the full set of AIRS channels and ideal and actual optimal channel subsets. Suboptimal retrieval scenarios—retrievals assuming a diagonal forward-model error covariance matrix and retrievals in the presence of Jacobian errors—are then examined.

a. Method

The a posteriori error covariance of an ensemble of linear minimum variance retrievals (\mathbf{A}) can be expressed analytically in terms of the a priori error covariance, observation error covariance, and Jacobian matrices. This is true both for statistically optimal retrievals and the suboptimal retrieval scenarios of interest here (Watts and McNally 1988; Collard 1999). Thus, the impact of radiative transfer model errors on retrieval accuracy can be assessed without performing the retrieval step per se. In this study a priori and a posteriori standard deviations for each element of the state vector are compared directly. Derived scalar figures of merit—the degrees of freedom for signal (the number of statistically independent pieces of information in any one measurement), and the measurement information content (a measure of the reduction of the volume of state space bounded by a given value of the probability density function, on assimilation of the observations; Rodgers 1996)—are also used to characterize retrieval accuracy.

A restricted but varied set of four profiles—two tropical profiles (ECMWF independent set profiles P002 and P012), a midlatitude profile (ECMWF independent set profile P007), and a high-latitude profile (dependent set profile P030)—have been analyzed. Results for profiles P002 and P030 documented here are characteristic of the full set and, notably, of humid/dry atmospheric state dependencies. Profile P030 is included specifically to assess the impact of Jacobian accuracy because maximum Garand measures of fit were noted for dry, high-latitude profiles.

A single a priori error covariance matrix \mathbf{B} —an ECMWF background error covariance matrix used in previous retrieval characterization studies (Collard 1999, 1998; Sherlock 2000a)—has been assumed in channel selection and impact studies. Results apply to retrievals/analyses in an operational context where the a priori estimate of atmospheric state is reasonably well constrained, particularly for the tropospheric temperature field.

Instrumental noise specifications and the forward-model error covariance matrix are as described in section 3. Reference Jacobians (for Jacobian error impact studies) were calculated using kCARTA.

b. Impact of forward-model errors on optimal linear retrievals

Retrieval errors for a perfect forward model ($\mathbf{F} = 0$, i.e., $\mathbf{R} = \mathbf{E}$) and actual forward-model errors ($\mathbf{R} = \mathbf{E} + \mathbf{F}$) are compared for profiles P002 and P030 in Fig. 7.

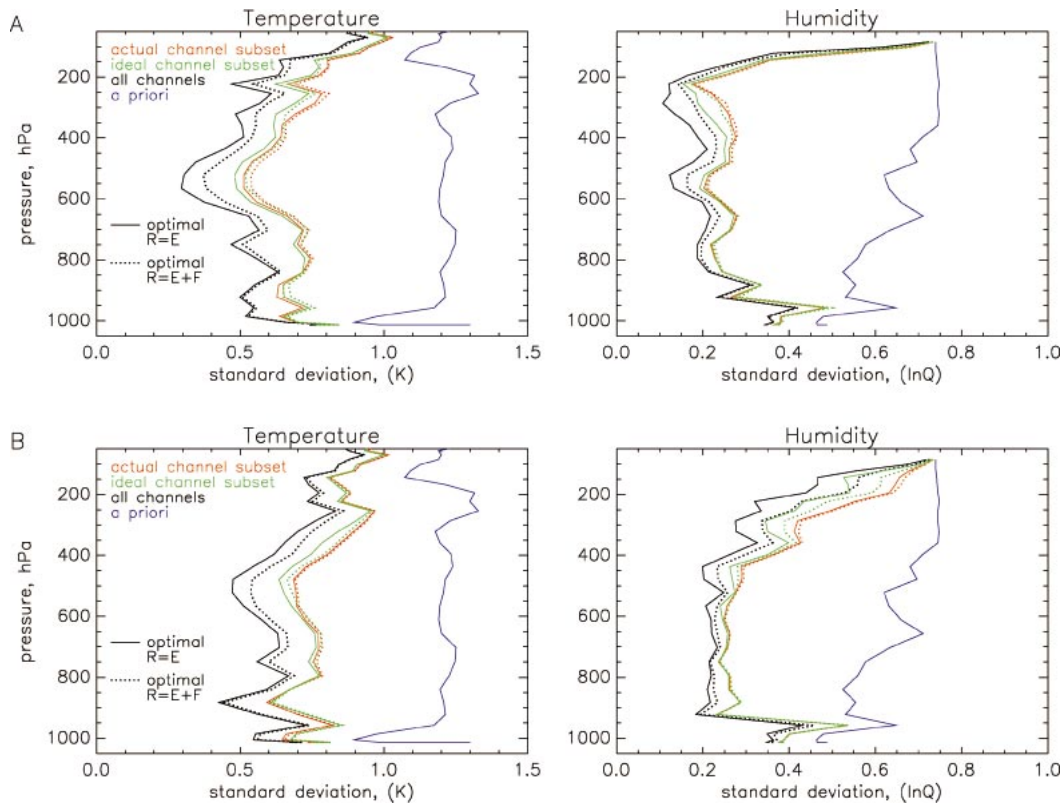


FIG. 7. Characterization of the impact of forward-model errors on retrieval accuracy for optimal retrievals of temperature and humidity (specifically, the logarithm of specific humidity, Q) for (a) tropical atmosphere P002 and (b) high-latitude atmosphere P030.

Forward-model errors in the $\text{H}_2\text{O } \nu_2$ band give a small but discernible reduction in the accuracy of tropospheric temperature and humidity retrievals using the full AIRS channel set. Maximum increases in the fraction of unexplained variance are observed for humidity retrievals above 300 hPa in the high-latitude atmosphere. Similar, but smaller, reductions in retrieval accuracy are observed for the ideal channel subset.

Forward-model errors modify the spectral sampling characteristics of the actual channel subset, leading to a loss of information in upper-tropospheric temperature and humidity retrievals. However, forward-model errors in selected channels have practically no impact on retrieval accuracy. Information loss is most significant in the high-latitude-atmosphere humidity retrievals (and to a lesser extent, temperature retrievals) above 300 hPa. Here the accuracy of actual channel subset retrievals is poorer than ideal channel subset retrievals, even when forward-model errors are taken into account.

Forward-model errors have essentially no impact on stratospheric temperature retrievals. Small changes in retrieval errors in the upper stratosphere associated with the shift in sampling to the CO_2 bands are noted, but their impact on the fraction of unexplained variance is negligible (a priori errors are on the order of 2–5 K). No significant changes in retrieval accuracy result from

the suboptimal retrieval scenarios considered here. Stratospheric temperature retrievals will not be discussed further.

Corresponding degrees of freedom for signal (dfs) and measurement information content are tabulated in the first two columns of Table 3. Forward-model errors typically lead to the loss of about 2 dfs and 5–10 bits of information for retrievals with the full AIRS channel set, about 1 dfs and 2–4 bits of information for retrievals with the ideal channel set, and 0.2 dfs and 1–2 bits of information for retrievals with the actual channel set. When forward-model errors are taken into consideration, the information contents of the two channel subsets are comparable; however, the degrees of freedom for signal associated with the actual channel set are 0.5–1 lower than those for the ideal channel set. Even when forward-model errors are taken into account, the number of independent pieces of information is greater for optimal retrievals using the ideal channel subset.

c. Suboptimal retrieval assuming a diagonal observation error covariance matrix

Retrieval errors will increase if a suboptimal gain matrix is assumed for retrievals. Characteristic errors for suboptimal retrievals in which a diagonal approxi-

TABLE 3. Degrees of freedom for signal (dfs) and measurement information content (Info, in bits, base e) for full, ideal, and actual channel subsets, in a range of optimal and suboptimal retrieval scenarios. Atmospheric states are identified by their dataset profile number, Pnm .

Scenario	Optimal $\mathbf{R} = \mathbf{E}$		Optimal $\mathbf{R} = \mathbf{E} + \mathbf{F}$		Suboptimal \mathbf{R} Diagonal \mathbf{F}		Suboptimal H' Full \mathbf{R}		Suboptimal H' Diagonal \mathbf{R}	
	Dfs	Info	Dfs	Info	Dfs	Info	Dfs	Info	Dfs	Info
P002 full	27.2	77.0	24.9	68.9	8.5	59.6	15.7	60.7	5.1	60.5
P002 ideal	20.9	51.6	19.7	47.7	19.0	46.3	18.0	45.5	17.5	45.6
P002 actual	19.5	51.0	19.1	48.0	19.0	47.5	18.4	46.3	18.3	47.0
P030 full	22.1	52.9	20.1	47.2	8.8	41.0	15.2	43.2	14.0	43.3
P030 ideal	16.7	34.8	15.7	32.6	15.1	31.6	13.9	31.1	13.9	31.5
P030 actual	15.1	33.5	14.9	32.3	14.8	32.0	14.4	31.7	14.4	32.2

mation is made to \mathbf{F} —and, hence, to the observation error covariance matrix—are illustrated in Fig. 8a. Optimal retrieval errors are traced for reference.

The diagonal approximation has negligible impact on retrieval errors for the actual channel subset but has a large impact for retrievals using the full AIRS channel set. In this case, ignoring interchannel error correlations leads to errors in upper-tropospheric temperature and humidity and boundary layer humidity that are comparable to or exceed errors in the a priori estimate of atmospheric state. For these regions, assimilation of data has no benefit and may even be detrimental. Tests demonstrate that the degradation in retrieval accuracy is due to the error correlations between channels in water vapor line centers where forward-model errors make the dominant contribution to the observation error covariance matrix, as expected.

Because the ideal channel subset includes more channels in water vapor line centers, retrieval errors are more sensitive to the specification of the observation error covariance matrix. Suboptimal retrieval errors are comparable to the errors illustrated for the the actual channel subset and are not included in Fig. 8a, for reasons of clarity.

Corresponding dfs and information content are tabulated in the third column of Table 3. There is a marked reduction (~ 10 – 20 dfs and 10 – 20 bits of information) for suboptimal retrievals using the full AIRS channel set. More modest reductions of 0.5 dfs and 1 – 1.5 bits of information are found for suboptimal retrievals using the ideal channel subset; reductions of 0.1 dfs and 0.2 – 0.5 bits of information are found for the actual channel subset. In the suboptimal retrieval scenario, the dfs (and effective retrieval-error standard deviations) are comparable for the ideal and actual channel subsets, and the information content of the actual channel subset tends to be 0.5 – 1 bits higher.

It may appear paradoxical that the suboptimal retrieval scenario with the maximum information content has the minimum degrees of freedom for signal, but this result can be readily understood. Information content (Info) and dfs can be expressed in terms of the eigenvalues λ_i of the matrix \mathbf{AB}^{-1} : $\text{Info} = -1/2 \ln(\prod \lambda_i)$ and $\text{dfs} = \sum 1 - \lambda_i$. Consideration of a simple two-

component system and two measurement scenarios (scenario a: $\lambda_1 = 0.01$ and $\lambda_2 = 0.9$ and scenario b: $\lambda_1 = 0.05$ and $\lambda_2 = 0.8$) suffices to show that the retrieval with the highest information content will not necessarily have the highest number of degrees for signal.

In suboptimal retrievals with the full AIRS channel set, the minimum eigenvalues of \mathbf{AB}^{-1} remain an order of magnitude smaller than those for retrievals using selected channel subsets, and this fact dominates in the estimation of information content. However, there is significant reduction in accuracy in the retrieval of many modes [in some cases the retrieval may be worse than the a priori estimate ($\lambda_i > 1$)] for suboptimal retrievals with the full AIRS channel set, leading to a significant reduction in the dfs. In fact these results suggest dfs rather than information content may be the most appropriate scalar figure of merit to optimize for channel selection.

d. Suboptimal retrieval due to Jacobian errors

Retrieval errors will also be increased if modeled Jacobians are in error. Optimal and suboptimal retrieval errors for the P002 and P030 atmospheres are illustrated in Figs. 8b and 8c, respectively. The impact of full and diagonal specifications of the observation error covariance matrix has been examined. Results are illustrated with dotted and dashed lines, respectively.

Jacobian errors have little impact on retrieval accuracy for the actual channel subset, although there is a small decrease in retrieval accuracy for upper-tropospheric humidity for the high-latitude atmosphere. There is no significant change in error characteristics with observation error covariance specification.

Jacobian errors do have a significant impact on retrieval accuracy for the full AIRS channel set—errors in modeled Jacobians degrade temperature and humidity retrievals throughout the troposphere. Moreover, error characteristics are sensitive to the specification of the observation error covariance matrix, particularly for the tropical atmosphere: when forward-model error correlations are neglected, the impact of Jacobian errors on retrieval accuracy is much greater.

Because it is perhaps unintuitive, we note that in-

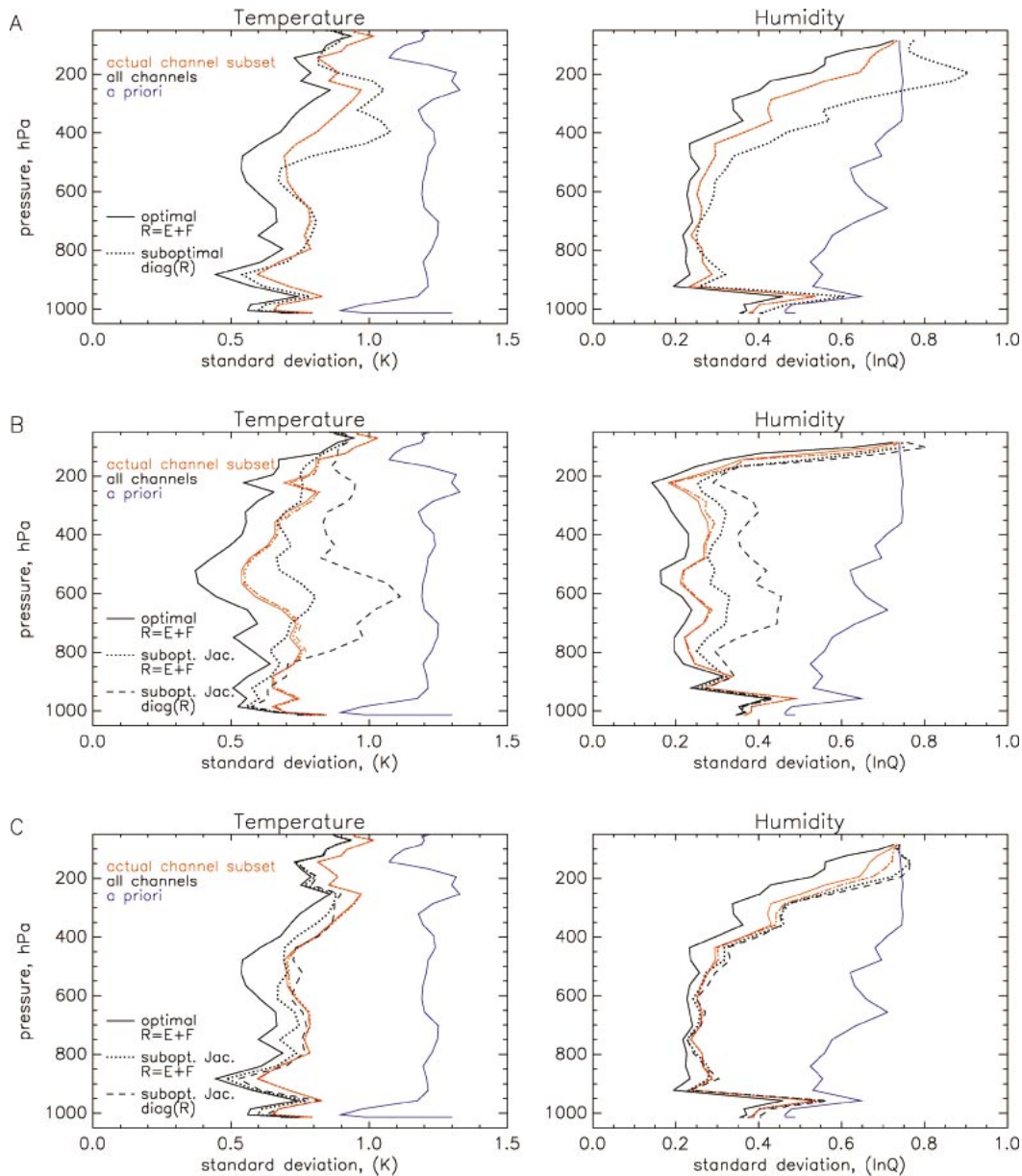


FIG. 8. Characterization of retrieval accuracy for suboptimal retrieval scenarios. (a) Impact of a diagonal approximation to the full observation error covariance matrix, high-latitude profile P030. (b) Impact of errors in modeled Jacobians on retrieval accuracy, tropical profile P002. Associated Garand measures of fit for humidity Jacobians are ≤ 15 for the full AIRS channel set and ≤ 10 for the actual channel subset. (c) Impact of errors in modeled Jacobians on retrieval accuracy, high-latitude profile P030. Associated Garand measures of fit for humidity Jacobians are ≤ 20 (exceptionally 40) in the longwave window region and ≤ 20 in the $\text{H}_2\text{O } \nu_2$ band for the full AIRS channel set. Garand measures of fit for humidity Jacobians are ≤ 20 in the longwave window region and ≤ 10 in the $\text{H}_2\text{O } \nu_2$ band for the actual channel subset.

creases in temperature errors are in fact due to errors in modeled humidity Jacobians—errors in modeled temperature Jacobians have essentially no impact on retrieval accuracy. Errors in humidity Jacobians affect temperature retrievals because of the fundamental ambiguity in partitioning the temperature and humidity signatures for radiance differences in the $\text{H}_2\text{O } \nu_2$ band: radiance differences due to differences in a priori and

true humidity profiles are mapped into temperature and humidity increments in the retrieval step, and vice versa.

As before, because the ideal channel subset samples more water vapor lines where errors in modeled absorption are high, retrieval accuracy is more sensitive to Jacobian errors. Suboptimal retrieval accuracy is generally comparable for the ideal and actual channels' subsets for temperature, whereas upper-tropospheric hu-

midity retrievals are slightly poorer using the ideal channel subset. There are also slightly larger increases in errors associated with the diagonal specification of the observation error covariance, although they are not of practical significance. Degrees of freedom for signal and measurement information content for suboptimal retrievals with full and diagonal specifications of the observation error covariance matrix are tabulated in Table 3 for reference.

5. Summary discussion

With the exception of channels in water vapor absorption line centers and some isolated spectral intervals with multiple interfering absorbers, the Gastropod model gives accurate and robust radiative transfer calculations. Forward-model errors are significantly less than AIRS instrumental noise specifications and are lower than noise levels recorded during laboratory performance characterization tests. Error inflation is modest (<30%) on passing from the dependent to independent set, even in instances in which there is a local extrapolation of the regression relations, and errors do not generally exhibit any marked satellite view angle or atmospheric state (latitude) dependencies. Garand measures of fit for temperature Jacobians are less than 10 for all profiles in the dependent set. Humidity Jacobians are modeled slightly less well: although the upper quartile for the Garand measure of fit is less than 10, maximum measures of fit range between 20 and 40. Errors in modeled water vapor line absorption make a significant contribution to diagonal and off-diagonal elements of the observation error covariance matrix, particularly at wavenumbers less than 1400 cm^{-1} . Associated Jacobian measures of fit generally range between 5 and 40.

Based on the linear minimum variance retrieval analysis, we would expect Gastropod forward-model errors to have little direct impact on the accuracy of operational retrievals using channel selections based on actual forward-model errors (the actual channel subset). No significant enhancement in retrieval error would be expected if a diagonal approximation was made to the full observation error covariance matrix, nor are Jacobian errors expected to have a significant impact on retrieval accuracy.

Gastropod forward-model errors do limit the spectral sampling characteristics of this selected channel subset in the $\text{H}_2\text{O } \nu_2$ band, resulting in a loss of information for upper-tropospheric temperature and humidity. However, when realistic suboptimal retrieval effects (diagonal approximation to the observation error covariance matrix, Jacobian errors) are taken into account, retrievals using the actual channel subset are expected to be more accurate than those using the ideal channel subset. Thus, in the case of the Gastropod model there is probably a small gain in accuracy to be made if actual for-

ward-model errors are taken into account in channel selection, although it is not essential to do so.

Errors in modeled water vapor absorption in line centers are expected to reduce the accuracy of optimal tropospheric temperature and humidity retrievals using the full AIRS channel set. In suboptimal retrieval scenarios, model errors are generally expected to degrade retrieval accuracy in the troposphere to levels comparable with the 130-channel subsets and, in some cases, may degrade accuracy to the point that there is no benefit to data assimilation.

Results indicate that an accurate description of forward-model-error correlations will be essential where forward-model errors make a significant contribution to the observation error covariance matrix: neglecting forward-model-error correlations was shown to affect retrieval accuracy through the propagation of both observation errors and correlated Jacobian errors into the retrieved estimate of atmospheric state.

Forward-model errors have been compared with an equivalent error characterization for the fixed-pressure-grid RTTOV-7 AIRS fast model. Forward-model errors are comparable to those reported for RTTOV-7 for fixed gas absorption and for water vapor absorption in the atmospheric window regions. RTTOV-7 performance in the $\text{H}_2\text{O } \nu_2$ band is significantly poorer: forward-model errors are comparable to instrumental noise levels in all channels in the $1400\text{--}1600\text{ cm}^{-1}$ interval.

The implications for retrievals of mid- and upper-tropospheric temperature and humidity using RTTOV-7 are threefold. Increased forward-model errors between absorption lines, comparable to instrumental noise levels, will reduce retrieval accuracy. These increases are likely to be associated with increased Jacobian errors and increased levels of interchannel error correlation within the $\text{H}_2\text{O } \nu_2$ band. Reductions in retrieval accuracy associated with suboptimal retrieval scenarios are, therefore, also expected to be greater.

Further improvements in FPG model descriptions of water vapor line absorption are, therefore, required if AIRS data are to be used to their full potential. Moreover, results presented here suggest that forward-model errors of less than 0.05 K are required, irrespective of instrumental noise levels, to ensure that Jacobians are modeled to required levels of accuracy. Forward-model errors of $\leq 0.05\text{ K}$ have been achieved with the hybrid FPG-FAO AIRS-RTA model.

Although there is every reason to believe that the retrieval impact analysis presented here will be representative of linear retrieval performance generally, the analysis should be extended to the full independent profile set and results should be summarized statistically. Further studies should be undertaken to characterize model performance—and to examine the impacts of Jacobian errors and diagonalization of \mathbf{R} on convergence—in a full nonlinear iterative retrieval framework, and analyses should be extended to more complete estimates of the forward-model error covariance matrix.

Nonetheless, the limited results presented here clearly show that it is essential to take suboptimal retrieval effects into account to make a realistic assessment of model performance and to provide useful guidance as to how the Gastropod model should be used in a non-linear iterative operational data assimilation algorithm.

6. Conclusions

Radiative transfer model errors have been characterized in detail for the Gastropod fixed-pressure-grid model. Forward-model-error characteristics do not compromise the information content of channel subsets appropriate for use in operational data assimilation significantly, and retrieval accuracy is robust to realistic, suboptimal retrieval scenarios. The regression model is, therefore, judged to be adequate for current operational data assimilation applications.

Errors in modeled water vapor line absorption limit the accuracy of retrievals using the full AIRS channel set, and accurate description of forward-model-error correlations between channels in water vapor line centers is essential for retrieval accuracy.

Thus, despite recent advances in modeling, fixed-pressure-grid fast models have yet to demonstrate adequate model accuracy for water vapor line absorption. Short of a major breakthrough in the regression models for water vapor line absorption, we do not foresee that significant improvements in performance will be achieved with fixed-pressure-grid schemes: the accuracy of regressions appears to be fundamentally limited by the magnitude of variability in water vapor abundances that must be modeled. It would appear that more complex models—the FAO or FPG–FAO hybrid methods developed specifically to address this problem, for example—will be required to exploit advanced sounder data to its full potential. Even then, many issues, notably, validation of spectroscopic parameter estimates and appropriate treatment of linearization errors, will need to be addressed before truly optimal use is made of information from water vapor line center absorption.

Acknowledgments. Thanks are given to Sergio De Souza-Machado for providing code and support for kCARTA, to John Eyre, Sean Healy, Michael Uddstrom, and Clive Rodgers for many useful discussions, to Marco Matricardi for permission to reproduce RTTOV-7 validation results, and to three anonymous referees for valuable comments that improved this paper. Author V. Sherlock's work at NIWA was funded under the Foundation of Research, Science, and Technology Contract C01X0032.

REFERENCES

- Aumann, H., and R. Pagano, 1994: Atmospheric infrared sounder on the Earth Observing System. *Opt. Eng.*, **33**, 776–784.
- Barnet, C. D., and J. Susskind, 1999: Simulation studies of advanced infrared and microwave sounders. *Proc. 10th Int. TOVS Study Conf.*, Boulder, CO, Bureau of Meteorology Research Centre, 22–33. [Available from the BMRC, P.O. Box 1289K, Melbourne, Victoria 3001, Australia.]
- Chalon, G., F. Cayla, and D. Diebel, 2001: IASI: An advanced sounder for operational meteorology. *Proc. 52d Int. Astronautical Federation Congress*, Toulouse, France, International Astronautical Federation. [Available from the IAF, 3-5 Rue Mario-Nikis, 75015 Paris, France.]
- Chevallier, F., 1999: Sampled databases of atmospheric profiles from the ECMWF 50-level forecast model. European Centre for Medium-Range Weather Forecasts Tech. Rep. SAF-RR-4, 21 pp. [Available from the Librarian, ECMWF, Shinfield Park, Reading RG2 9AX, United Kingdom.]
- Collard, A. D., 1998: Notes on IASI performance. Met Office Tech. Rep. FR-256, 20 pp. [Available from the National Meteorological Library, Fitzroy Road, Exeter EX1 3PB, United Kingdom.]
- , 1999: The effect of undetected cloud on IASI retrievals. Met Office Tech. Rep. FR-261, 23 pp. [Available from the National Meteorological Library, Fitzroy Road, Exeter EX1 3PB, United Kingdom.]
- Eyre, J., G. Kelly, A. McNally, E. Andersson, and A. Persson, 1993: Assimilation of TOVS radiance information through one-dimensional variational analysis. *Quart. J. Roy. Meteor. Soc.*, **119**, 1427–1463.
- Garand, L., D. S. Turner, C. Chouinard, and J. Hallé, 1999: A physical formulation of atmospheric transmittances for the massive assimilation of satellite infrared radiances. *J. Appl. Meteor.*, **38**, 541–554.
- , and Coauthors, 2001: Radiance and Jacobian intercomparison of radiative transfer models applied to HIRS and AMSU channels. *J. Geophys. Res.*, **106**, 24 017–24 032.
- Giering, R., and T. Kaminski, 1996: Recipes for adjoint code construction. Max-Planck-Institut für Meteorologie Tech. Rep. 212, 35 pp. [Available from the National Meteorological Library, Fitzroy Road, Exeter EX1 3PB, United Kingdom.]
- Hannon, S., L. L. Strow, and W. W. McMillan, 1996: Atmospheric infrared fast transmittance models: A comparison of two approaches. *Proc. SPIE*, **2830**, 94–105.
- Matricardi, M., and R. Saunders, 1999: Fast radiative transfer model for simulation of infrared atmospheric sounding interferometer radiances. *Appl. Opt.*, **38**, 5679–5691.
- , F. Chevallier, and S. Tjemkes, 2001: An improved general fast radiative transfer model for the assimilation of radiance observations. European Centre for Medium-Range Weather Forecasts Tech. Rep. 345, 40 pp. [Available from the Librarian, ECMWF, Shinfield Park, Reading RG2 9AX, United Kingdom.]
- McMillin, L., and H. Fleming, 1976: Atmospheric transmittance of an absorbing gas: Computationally fast and accurate transmittance model for absorbing gases with constant mixing ratios in inhomogeneous atmospheres. *Appl. Opt.*, **15**, 358–363.
- , ———, and M. Hill, 1979: Atmospheric transmittance of an absorbing gas. 3: A computationally fast and accurate transmittance model for absorbing gases with variable mixing ratios. *Appl. Opt.*, **18**, 1600–1606.
- , L. J. Crone, M. D. Goldberg, and T. J. Kleespies, 1995: Atmospheric transmittance of an absorbing gas. 4. OPTRAN: A computationally fast and accurate transmittance model for absorbing gases with fixed and variable mixing ratios at variable viewing angles. *Appl. Opt.*, **34**, 6269–6274.
- Morse, P., J. Bates, C. Millar, M. Chahine, F. O'Callaghan, H. Aumann, and A. Karnik, 1999: Development and test of the Atmospheric Infrared Sounder (AIRS) for the NASA Earth Observing System (EOS). *Proc. SPIE*, **3759**, 236–253.
- Predina, J., and R. Glumb, 2000: The Crosstrack Infrared Sounder (CrIS): Data algorithms and products. *Tech. Proc. 11th Int. ATOVS Study Conf.*, Budapest, Hungary, Bureau of Meteorology Research Centre, 293–305. [Available from the BMRC, P.O. Box 1289K, Melbourne, Victoria 3001, Australia.]

- Rodgers, C. D., 1996: Information content and optimisation of high spectral resolution measurements. *Proc. SPIE*, **2830**, 136–147.
- Saunders, R., 2000: Assimilation of AIRS and IASI data: Forward modelling. *ECMWF Seminar Proc., Exploitation of the New Generation of Satellite Instruments for Numerical Weather Prediction*, Reading, United Kingdom, European Centre for Medium-Range Weather Forecasts, 181–200.
- , P. Brunel, F. Chevallier, G. Deblonde, S. English, M. Matricardi, and P. Rayer, 2002: RTTOV-7 science and validation report. Met Office Tech. Rep. FR-387, 51 pp. [Available from the National Meteorological Library, Fitzroy Road, Exeter EX1 3PB, United Kingdom.]
- Sherlock, V., 2000a: Impact of RTIASI fast radiative transfer model error on IASI retrieval accuracy. Met Office Tech. Rep. FR-319, 37 pp. [Available from the National Meteorological Library, Fitzroy Road, Exeter EX1 3PB, United Kingdom.]
- , 2000b: Results from the first UKMO IASI fast radiative transfer model intercomparison. Met Office Tech. Rep. FR-287, 42 pp. [Available from the National Meteorological Library, Fitzroy Road, Exeter EX1 3PB, United Kingdom.]
- , 2001a: Gastropod—A fast radiative transfer model for the advanced sounders. Met Office Tech. Rep. FR-362, 37 pp. [Available from the National Meteorological Library, Fitzroy Road, Exeter EX1 3PB, United Kingdom.]
- , 2001b: Vertical discretisation for advanced sounder radiative transfer models: Grid refinement for RTIASI. Met Office Tech. Rep. FR-336, 32 pp. [Available from the National Meteorological Library, Fitzroy Road, Exeter EX1 3PB, United Kingdom.]
- , 2002: Improving fast radiative transfer model predictions of water vapour line absorption. *Tech. Proc. 12th Int. ATOVS Study Conf.*, Lorne, Australia, Bureau of Meteorology Research Centre, in press. [Available from the BMRC, P.O. Box 1289K, Melbourne, Victoria 3001, Australia.]
- , and R. Saunders, 2000: ISEM-6: Infrared surface emissivity model for RTTOV-6. *Tech. Proc. 11th Int. ATOVS Study Conf.*, Budapest, Hungary, Bureau of Meteorology Research Centre, 383–389. [Available from the BMRC, P.O. Box 1289K, Melbourne, Victoria 3001, Australia.]
- , A. Collard, and R. Saunders, 2002: Development and validation of Gastropod, a fast radiative transfer model for the advanced sounders. *Tech. Proc. 12th Int. ATOVS Study Conf.*, Lorne, Australia, Bureau of Meteorology Research Centre, in press. [Available from the BMRC, P.O. Box 1289K, Melbourne, Victoria 3001, Australia.]
- Simmons, A., and A. Hollingsworth, 2002: Some aspects of the improvement in skill of numerical weather prediction. *Quart. J. Roy. Meteor. Soc.*, **128**, 647–677.
- Strow, L. L., H. Motteler, R. Benson, S. Hannon, and S. D. Souza-Machado, 1998: Fast computation of monochromatic infrared atmospheric transmittances using compressed lookup tables. *J. Quant. Spectros. Radiat. Transfer*, **59**, 481–493.
- , S. E. Hannon, S. de Souza-Machado, H. E. Motteler, and D. Tobin, 2003: An overview of the AIRS radiative transfer model. *IEEE Trans. Geosci. Remote Sens.*, **41**, 303–313.
- Tjemkes, S., and Coauthors, 2003: The ISSWG line-by-line intercomparison experiment. *J. Quant. Spectrosc. Radiat. Transfer*, **77**, 433–453.
- van Delst, P., 2002: Upgraded radiative transfer model status at NCEP/EMC. *Tech. Proc. 12th Int. ATOVS Study Conf.*, Lorne, Australia, Bureau of Meteorology Research Centre, in press. [Available from the BMRC, P.O. Box 1289K, Melbourne, Victoria 3001, Australia.]
- Watts, P. D., and A. P. McNally, 1988: The sensitivity of a minimum variance retrieval scheme to the value of its principal parameters. *Proc. Fourth Int. TOVS Study Conf.*, Igls, Austria, Cooperative Institute for Meteorological Satellite Studies, 399–412. [Available from CIMSS, University of Wisconsin—Madison, 1225 W. Dayton St., Madison, WI 53706.]